Spectral hole burning of Eu^{2+} in CaF_2

D. M. Boye
Davidson College, Davidson, North Carolina 28036

R. M. Macfarlane
IBM Almaden Research Center, 650 Harry Road, San Jose, California 95120

Y. Sun and R. S. Meltzer
Department of Physics and Astronomy, University of Georgia, Athens, Georgia 30602

(Received 29 January 1996)

Spectral hole burning on the $4f^7(^8S_{7/2}) \rightarrow 4f^6 5d$ transition of Eu^{2+} is observed to occur by two mechanisms in CaF_2:Eu^{2+}. At zero magnetic field, persistent spectral hole burning occurs by two-step photoionization where the hole burning survives cycling to room temperature. The observed hole spectrum is compared with a calculation which considers the small Eu^{2+} ground-state splitting and both the ground- and excited-state hyperfine interactions. In a magnetic field above 1 T, transient spectral hole burning occurs by population redistribution among the ground-state hyperfine levels. Long-lived (minutes) holes are observed for a half integral spin system. The resulting hole spectrum consists of holes, antiholes, and a nuclear spin-flip sideband and can be explained from the hyperfine interactions in the ground and excited states. The dominant hole decay occurs by phonon-induced transitions among hyperfine levels of the $M_S = -7/2$ and $M_S = -5/2$ electron-spin sublevels. Central hole linewidths of 200 MHz are observed at zero magnetic field. Hole linewidths at high magnetic fields are as narrow as 40 MHz but these are inhomogenously broadened by superhyperfine interactions with the F nuclear spins. Estimates of hole-burning quantum efficiency are also obtained. [S0163-1829(96)05533-6]

INTRODUCTION

Optical hole-burning spectroscopy has been an effective tool to perform high-resolution spectroscopy in solids where the information of interest is buried in the optical inhomogeneous linewidth. Hole burning occurs when a frequency selected subset of the optically active species is modified in some way thereby altering the optical-absorption spectrum. Hole burning can occur by a variety of means[1] including photochemical removal of the species, modification of the optical transition frequency through changes in the environment, or storage of the selected population in either the electronic excited states or the hyperfine levels in the ground manifold of states.

In this paper we report high-resolution optical hole-burning experiments of Eu^{2+} in CaF_2. The spectroscopy of CaF_2:Eu^{2+} has been well-studied in absorption (and fluorescence),[2–5] electron-spin resonance,[6] electron nuclear double resonance,[7] and in optically detected magnetic resonance.[8] The ground state is the $^8S_{7/2}$ state of the $4f^7$ configuration which is split by the cubic field and spin-orbit coupling into a triplet spanning about 5.6 GHz. The excited state is a Γ_8 state of the $4f^6 5d$ configuration. The transition is parity allowed giving rise to strong transitions and a fluorescence decay lifetime at a temperature of 1.5 K of about 0.7 μs.[9] The spectrum in absorption and fluorescence consists of a zero-phonon line at 413.1 nm with a strong vibronic sideband.

CaF_2:Eu^{2+} exhibits photoconductivity when excited with photons of energy exceeding 3.8 eV.[10] This has been ascribed to photoionization of the excited Eu^{2+} ions where the electron is excited above the conduction band. This is consistent with the fact that the Eu^{2+} absorption can be bleached when strongly excited into the $4f^6 5d$ configuration.[11]

In this paper we perform optical hole burning on the zero-phonon line of the $4f^7(^8S_{7/2}) \rightarrow 4f^6 5d(\Gamma_8)$ transition of Eu^{2+} in CaF_2. We show that two mechanisms contribute to the hole burning. At zero magnetic field, photoionization leads to frequency selective removal of some of the Eu^{2+} ions. The resulting hole spectrum reflects the absorption spectrum of the removed ions and contains considerable structure which reveals the zero-field splitting of the $^8S_{7/2}$ ground state. The spectrum can be understood by considering this zero-field splitting and the hyperfine interactions in the ground and excited states of the two Eu isotopes. This is demonstrated with a calculation of the expected hole-burning spectrum considering the possible transitions among these hyperfine levels. As a result of the trapping of the photoionized electron, the hole burning is persistent. In a crystal double doped with Eu^{2+} and samarium, the traps are quite deep as the holes survive 5 min of cycling to 300 K.

In a large magnetic field the dominant mechanism for hole burning is population redistribution among the hyperfine levels in the ground state of the two Eu isotopes. Although the holes are transient, their lifetime can be of the order of minutes at a temperature of 2 K in fields above 5 T. We show that the resulting spectrum is determined by the hyperfine splittings in the ground and excited states. A study of the temperature dependence of the hole lifetime indicates that the nuclear-spin relaxation occurs by thermally induced electron-spin transitions among the ground-state electron-spin levels which are accompanied, on occasion, by nuclear spin flips.

EXPERIMENT

Burning and detection of the holes were performed with an actively stabilized, frequency-doubled Ti:sapphire laser, Coherent 899-21, having a linewidth of ≈1 MHz in the near infrared and 2 MHz doubled. Doubling was accomplished with an intracavity frequency doubler system. The doubled output was focused to a spot size of ~50 μm with a depth of field of about 1.5 mm. Using output powers of up to 1 mW, the maximum burn intensity was about 50 W/cm^2.

Holes were probed by monitoring the fluorescence as the laser was scanned by up to ±10 GHz. Photoionization holes were burned with intensities of about 50 W/cm^2 and were probed at about 1 W/cm^2. For the hole-burning experiments in a magnetic field, burning and scanning were both done with intensities of less than 1 W/cm^2.

Scanning was performed by applying a voltage ramp, with a typical period of 100 ms, to a thin intracavity tipping plate in the laser cavity. For the persistent hole burning, the hole spectra were obtained by averaging about 256 scans. For the transient holes obtained in a magnetic field, the hole lifetime was not sufficiently long to perform an adequate number of averages. Therefore a burn-scan sequence was used where during the period between each scan the laser frequency was returned to its initial position to reburn the hole for about 100 ms.

For the zero-field experiments, the sample was immersed in pumped liquid helium for temperatures between 1.5 and 4.2 K. For higher temperatures, cold helium gas was flowed past the crystal by permitting helium to pass from the main reservoir to the sample chamber through a capillary tube and valve. For experiments in a magnetic field, the samples was mounted on a cold finger centered within a superconducting magnet. In order to provide the lowest possible temperatures, the sample was surrounded by a copper radiation shield with a quartz window which was in good thermal contact with the main liquid-helium reservoir at 4.2 K. Even so, the sample temperature was higher than that of the helium bath. Past experience with other samples mounted in a similar fashion indicate that the temperature of the sample was about 0.5–1 K above that of the helium chamber to which the cold finger was attached. Since the coil had only axial access, the burn and probe laser beam entered the cryostat through the same window at the bottom of the cryostat as the detected fluorescence. Corning 3-73 and 7-59 filters were used to block the scattered laser radiation but transmit the fluorescence in the range from 420–480 nm.

RESULTS

A. Zero-field hole burning

With a tightly focused laser tuned to the 413 nm zero-phonon line (ZPL), shallow holes could be burned after about 10 min with a power density of about 1 W/cm^2. A typical spectrum, burned for 75 min, is shown in Fig. 1. The spectrum has several noteworthy features. At the laser frequency is a narrow central feature whose linewidth is about 200 MHz in a sample with 0.001% Eu^{2+}. Also centered on the laser frequency is a broader pedestal whose width is about 1.5 GHz. On either side of the central hole, split off by about 2.5–3 GHz, is a clearly defined sidehole. An indication

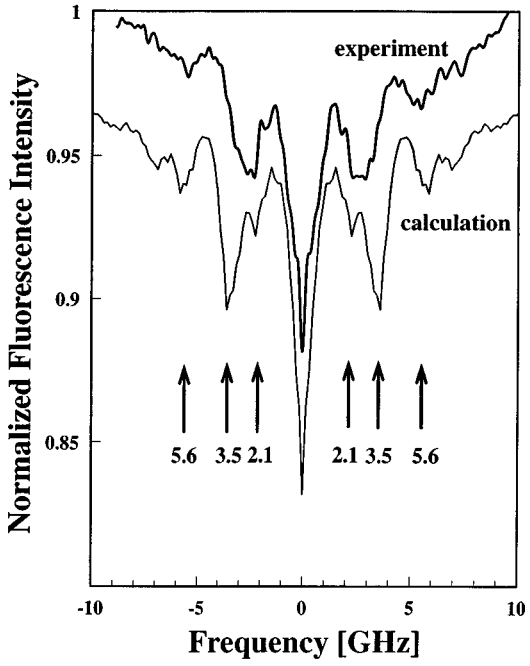

FIG. 1. Spectrum of the hole burned with a power of 50 W/cm^2 for 75 min in the $4f^7(^8S_{7/2}) \rightarrow 4f^6 5d(\Gamma_8)$ zero-phonon transition of Eu^{2+} (0.001%) in CaF_2 at 1.5 K. The lighter curve describes the calculated spectrum described in the text.

of a second sidehole at 5.5 GHz is also seen on either side of the central features. The sideholes have widths similar to that of the central pedestal. The maximum hole depth at the narrow spectral feature is about 10%.

If the holes are burned for longer times the maximum depth can approach about 15% but the central feature becomes slightly broadened. The sideholes remain relatively unchanged aside from a proportional increase in depth.

Holes could be burned over most of the inhomogeneously broadened (40 GHz) ZPL in the 0.001% sample. However the resulting holes were shallower on the high-frequency portion of the ZPL. In the 0.1% sample holes could only be burned on the lower energy side of the ZPL and the central feature was somewhat broader than in the 0.001% sample. Otherwise the hole spectrum looked similar in the two samples. The dependence of the hole burning on position within the inhomogeneously broadened line suggests the interesting possibility that a correlation may exist between transition frequency and the availability of nearby electron traps.

B. Hole burning in a magnetic field

In a magnetic field above 1 T, only transient holes were observed. The mechanism for the hole burning in a field is therefore quite different. In a field, holes could be burned in less than 100 ms with 1 W/cm^2 of focused laser power and a much greater hole depth could be achieved. This is illustrated in Fig. 2 for a field of 7.7 T where the fluorescence intensity, which is proportional to the absorption, is plotted as a function of time after the initiation of illumination of the sample. As the field is decreased the hole depth decreases because, as we will show, the hole lifetime becomes shorter. An increase in temperature also reduces the hole depth as

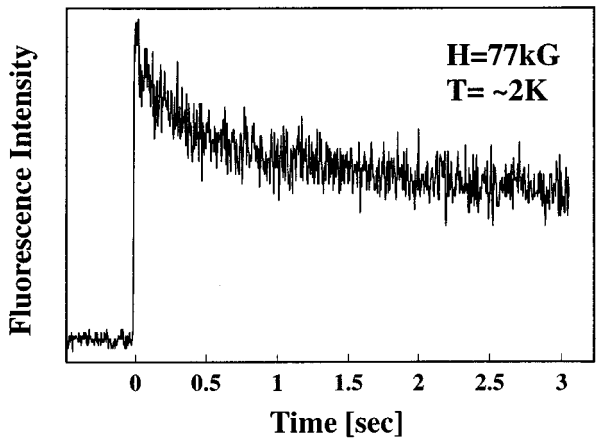

FIG. 2. Burning curve for the $4f^7(^8S_{7/2})\rightarrow 4f^6 5d(\Gamma_8)$ zero-phonon transition of Eu^{2+} (0.001%) in CaF_2 with 1 W/cm^2 in a field of 7.7 T.

this also reduces the hole lifetime. The temperature dependence of the maximum hole depth is shown in Fig. 3 for a field of 3.8 T. The hole-burning conditions were such that deep ($\cong$50%) holes could be burned in about 1 s at 2 K.

Hole spectra at several fields and at a temperature of 2 K are shown in Fig. 4. Most of the features in the spectrum are nearly independent of field except for the two narrow sideholes on either side of the central feature. The field-independent sideholes are always broader and shallower than the central hole. The splitting of the field-dependent sidehole from the central hole is linear in field as demonstrated in Fig. 5.

The width of the central hole is somewhat a function of the hole depth. For hole depths below about 20%, the linewidth reduces to about 40 MHz and is independent of hole depth. For fields between 3 and 8 T the hole width of the central feature was independent of field. Similarly, the hole width was temperature independent between 2 and 4 K. For fields below 3 T and temperatures above 4 K, the hole spectra were not of adequate quality to obtain a reliable linewidth.

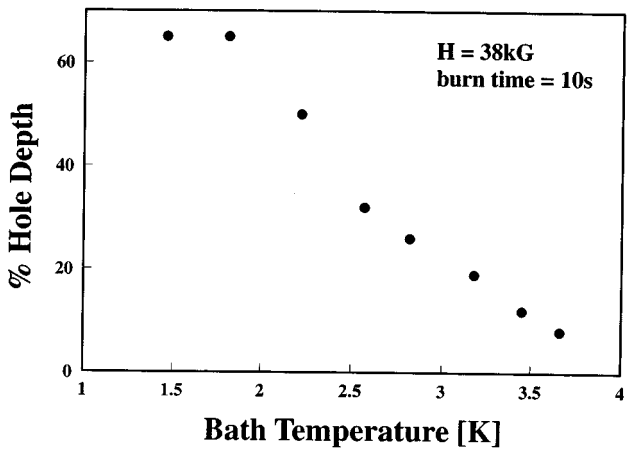

FIG. 3. Hole depth as a function of the temperature at a time 0.5 s after the end of a 10 s burn at 1 W/cm^2 in a field of 3.8 T.

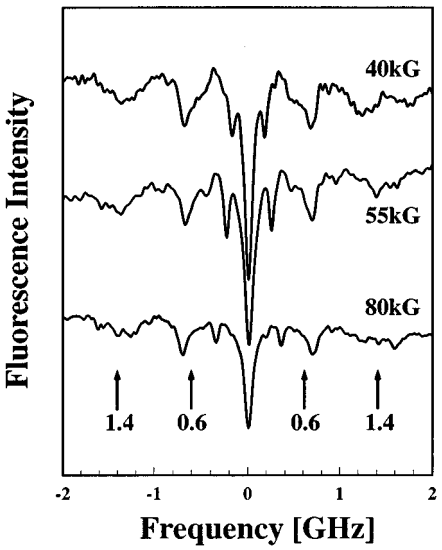

FIG. 4. Magnetic-field dependence of the population hole-burning spectrum of the $4f^7(^8S_{7/2})\rightarrow 4f^6 5d(\Gamma_8)$ zero-phonon transition of Eu^{2+} (0.001%) in CaF_2 at 2 K.

DISCUSSION

Zero-field hole spectrum

It is well-known, from electron-spin resonance, that the ground state of Eu^{2+} is split into a triplet by the combined action of the cubic crystalline field and spin-orbit coupling. Because of the nearly pure spin character of the $^8S_{7/2}$ ground state, this splitting is very small. Although the splitting at zero field has never been directly observed, EPR spectra at a field of several kilogauss have been fitted to a ground-state spin Hamiltonian[7] which at zero-field would have a twofold degenerate Γ_7 representation lowest with a fourfold degenerate Γ_8 level at 3.5 GHz and a twofold Γ_6 level 5.6 GHz above the Γ_7 ground state. This is indicated on the left in Fig. 6. In addition, the hyperfine interaction of the Eu^{2+} electron spin with the $I=5/2$ nuclear spin of the ^{151}Eu and ^{153}Eu isotopes further breaks up the degeneracy.

The resulting Hamiltonian for the ground state, keeping only those terms of sufficient magnitude to contribute to the

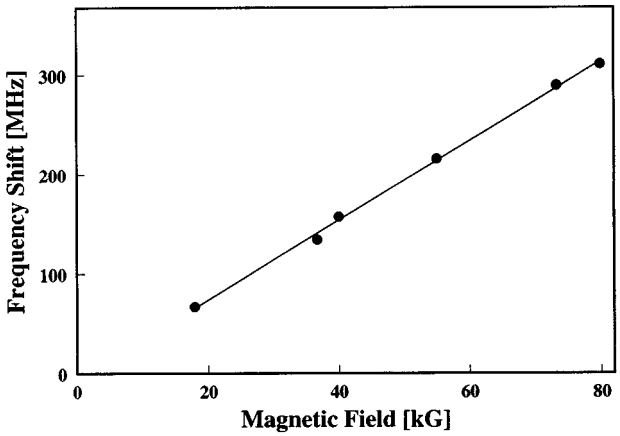

FIG. 5. Magnetic-field dependence of the field-dependent sideholes of the $f^7(^8S_{7/2})\rightarrow 4f^6 5d(\Gamma_8)$ zero-phonon transition of Eu^{2+} (0.001%) in CaF_2.

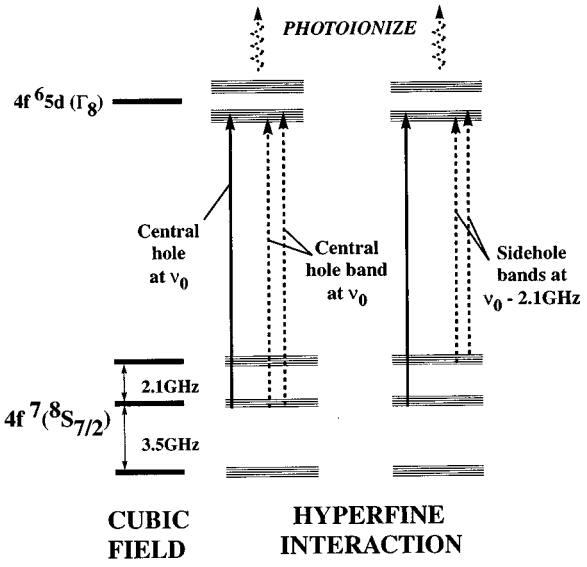

FIG. 6. Schematic of energy levels of the $^8S_{7/2}$ ground state and Γ_8 excited state of Eu^{2+} in CaF_2. The solid vertical arrow indicates the central hole on an ion in resonance with the laser frequency which results when photoionization occurs by excited-state absorption. The dotted arrows indicate some of the other transitions which are absent after photoionization has occurred producing the broad central hole and sideholes.

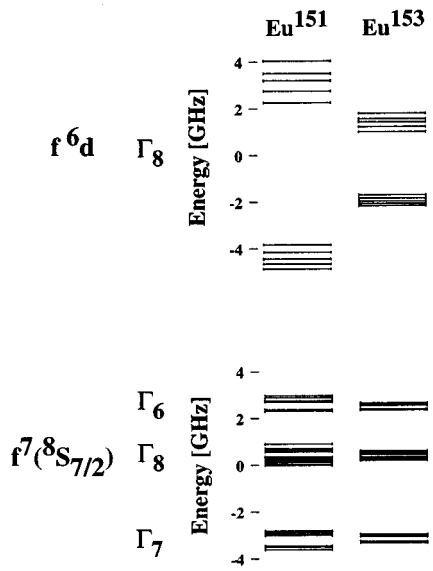

FIG. 7. Ground- and excited-state splitting of Eu^{2+} in CaF_2 calculated with Eqs. (1) and (2) and the parameters in Table I.

spectrum as resolved in the hole-burning experiments, is, according to Baker and Williams[7]

$$H_{\rm gr}=g_{\rm gr}\beta\mathbf{H}\cdot\mathbf{S}+B_4(O_4^0+5O_4^4)+A_{\rm gr}\mathbf{I}\cdot\mathbf{S}, \qquad (1)$$

where $g_{\rm gr}$ is the ground-state g value, close to 2, $\mathbf{H}$ is the magnetic field, $\mathbf{I}$ and $\mathbf{S}$ are the electron- and nuclear-spin operators, respectively, and the O_k^q are operator equivalents which are found in Abragam and Bleaney.[12] The O_4^4 term couples states of $\Delta M_S=\pm 4$. Sixth rank terms containing operators O_6^q have been omitted because the very small values obtained from the fits of the ground-state resonance spectra lead to the conclusion that they make negligibly small contributions to the hole spectrum. There are a total of 8(electron spin)×6(nuclear spin)=48 basis states. The resulting matrix breaks up into four 12×12 matrices, two of which are degenerate. The parameters that were obtained by Baker and Williams[7] from fitting the electron nuclear double resonance spectrum at 9.1 GHz are shown in Table I and these were used to solve for the eigenvalues of the spin Hamiltonian at zero field. The resulting ground manifold of states for the two Eu isotopes are shown in Fig. 7.

The lowest excited state is a Γ_8 electron-spin quartet. When this is coupled to the six nuclear-spin states of $I=5/2$, there results a 24×24 matrix to solve. The spin Hamiltonian for a Γ_8 is written using an effective spin $S=3/2$ of the form[13]

$$H_{\rm ex}=\beta\Sigma_{i=x,y,z}(gH_iS_i+fH_iS_i^3)+A_{\rm ex}\Sigma_{i=x,y,z}(gI_iS_i+fI_iS_i^3), \qquad (2)$$

where the first term accounts for the anisotropic Zeeman interaction and the second the anisotropic hyperfine interaction. For zero field the first term is zero. The parameters for the excited state are known from the microwave optical double-resonance experiments of Chase.[8] The parameters g and f in Eq. (2) are related to γ and δ given by Chase[8] through the relations

$$\gamma=g+1.75f \quad \text{and} \quad \delta^2=f(g+5f/2) \qquad (3)$$

and are listed in Table I.

The resulting zero-field hyperfine energy levels for the Γ_8 excited state are also shown in Fig. 7 for the two Eu isotopes.

TABLE I. Parameters used for the Hamiltonian of Eqs. (1) and (2) and comparison with previously obtained values.

	This work	Ref. 7	Ref. 8	Ref. 5
60 B_4 (MHz)	173.7	176.12		
$A_{\rm gr}[^{151}{\rm Eu}, ^{153}{\rm Eu}]$ (MHz)	−102.9, −45.7	−102.91, −45.67		
δ^2	4.84		4.43	4.11
γ^2	0.16		0.045	0.125
$\lvert f\rvert$[a]	2.821		2.57	2.59
$\lvert g\rvert$[a]	5.337		4.71	4.88
$A_{\rm ex}[^{151}{\rm Eu},^{153}{\rm Eu}]$ (MHz)	650, 289			

[a]The values of f and g have opposite sign.

For the parameters obtained by Chase[8] for the ^{151}Eu (^{153}Eu) isotopes, the energy levels form two groups separated by about 7 (3) GHz, where each group is rather tightly clustered with an energy spread for the lower group of about 0.6 (0.25) GHz and for the upper group 1.0 (0.4) GHz.

The hole-burning spectrum is calculated by allowing photoionization to occur for those ions which have one of their transitions between the 48 ground-state hyperfine levels and the 24 excited-state levels in resonance with the laser frequency. Each ion then contributes its full spectrum to the hole spectrum since all the transitions of that ion are now removed from the absorption spectrum. However the spectrum of all possible transitions from each ion contributing to the hole spectrum is shifted from one another since the optical transition which selectively led to photoionization must occur at the laser frequency. Several examples showing the mechanisms for the creation of the central and sideholes are indicated in Fig. 6. The fact that all ions contribute to the hole at the laser frequency leads to a narrow central feature in the hole spectrum at that frequency.

In the calculation, we assume that all transitions are equally probable to be in resonance with the laser since the inhomogeneous linewidth (40 GHz) is much greater than any of the splittings in the ground or excited states. Although the selection rule $\Delta m_I=0$ should be obeyed, the resulting zero-field eigenvectors contain an admixture of many of the m_I states. In addition, since the electronic part of the wave function of the excited state is not known from the solution to the effective spin-Hamiltonian, the relative strengths among the levels still could not be determined. Therefore, while all transitions do not have equal transition probabilities, transitions will occur between some members of all three groups of levels in the ground state to some members of the two groups of levels in the excited state. Since the splittings within each of these groups is smaller than the linewidths of the observed hole spectrum, the assumption of equal transition probability should provide a reasonable first approximation to the spectrum.

The hole spectrum is then calculated from the sum of all transitions for ions selectively photoionized on each of the possible transitions. This is done for both Eu isotopes, each contributing according to its isotopic (nearly equal) abundance. The excited-state parameters were varied to give a best fit to the observed hole spectrum. They are compared in Fig. 1. The best-fit excited-state parameters are similar to those of Kisliuk, Tippens, and Moore[5] and that of Chase[8] as can be seen in Table I. The calculation exhibits all of the main features of the observed spectrum at the appropriate relative transitions energies. The calculations yield a greater intensity for the outer edge of the first sideholes whereas the measured first sideholes have a greater intensity on the inner edge. In addition the calculated linewidths are somewhat narrower than those of the observed spectrum. Nonetheless, the agreement is surprisingly good considering the assumptions in the calculation. These include the use of equal transition intensities, the omission of effects of strain and the neglect of vibronic coupling. Chase[8] has shown that strain and vibronic coupling are important in understanding the microwave optical double resonance of the excited state. The good fit occurs because the dominant features of the spectrum result from the ground-state energy-level structure which is insensitive to both of these effects.

Hole spectrum in a field

The calculation of the hole spectrum in a large magnetic field (>3 T) is somewhat more straightforward. Since the ground state is a nearly pure $S=7/2$ electron-spin system with an isotropic g value of 2, the energy levels are organized into eight groups determined by M_S. The hyperfine term in Eq. (1) leads to a subgroup of six hyperfine levels for each electronic Zeeman level with a nearly equal splitting between the six levels of M_SA. At 2 K, only the hyperfine levels of the $M_S=-7/2$ state are significantly occupied. Since $M_SA \ll kT$, the occupations of the six hyperfine levels in thermal equilibrium are essentially equal.

In a magnetic field, the excited state is split into four groups based on the four components of the $S=3/2$ effective spin, each group containing six nearly equally spaced hyperfine levels. Because of the anisotropy of the Hamiltonian of Eq. (2), the Zeeman and hyperfine splittings depend on the orientation of **H**. The exact splitting is obtained from a solution of the Hamiltonian of Eq. (2) where in these experiments **H** is directed 12° from the [111] direction with direction cosines, −0.41, 0.54, and 0.73 with respect to the fourfold axis. The hyperfine splittings of the excited state are about a factor of 5 greater than those of the ground state. According to the parameters obtained from the microwave optical double-resonance results of Chase,[8] the hyperfine splittings at high fields for ^{15}Eu (^{153}Eu) are 1.4 (0.6) and 1.0 (0.4) GHz for the outer and inner electronic Zeeman levels, respectively, for H directed as described above. The ground- and excited-state energy levels are schematically indicated in Fig. 8.

Hole burning in a large magnetic field occurs by population redistribution among the hyperfine levels. Although M_S and m_I are nearly good quantum numbers, the ground- and excited-state Hamiltonians still admit a small remnant admixture which allows optical transitions of $\Delta M_S \neq 0$ and $\Delta m_I \neq 0$ with a small probability. As a result, in the cycle of excitation and relaxation, ions can return to hyperfine levels of the $M_S=-7/2$ ground state which are different from that from which they originated. If the relaxation among hyperfine levels is sufficiently slow, significant population redistribution can occur giving rise to a reduction of population of those states of an ion which have transitions in resonance with the laser and enhancement of populations of other hyperfine levels of the ion. This results in a hole in the spectrum and sideholes at frequencies given by the excited-state splitting. In addition, antiholes may occur at frequencies shifted from the laser frequency by differences in the ground- and excited-state splittings.

Applying these predictions to the observed spectra, we associate the sideholes at 0.6 and 1.4 GHz with the hyperfine splittings of the lower Zeeman level of the excited state. At some fields, an antihole is observed at 0.35 GHz which is assigned to the ground-state hyperfine splitting of the ^{151}Eu isotope. The hyperfine splitting of the ^{153}Eu isotope is too small to be resolved. Transitions from the $M_S=-7/2$ ground-state electron-spin level to the higher-lying Zeeman

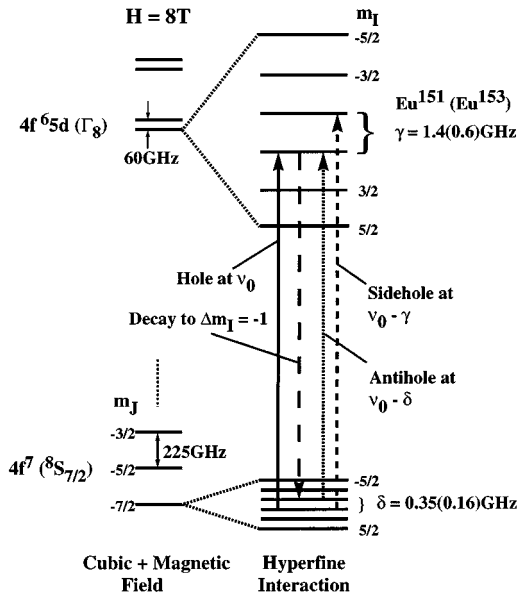

FIG. 8. Schematic of energy levels of ground and excited states of Eu^{2+} in CaF_2 in a field of 8 T. The solid arrow indicates the transition at the laser frequency which produces the central hole. The downward dashed arrow shows the decay to a different ground-state hyperfine level producing a population redistribution. The two upward arrows show the resulting sidehole and antihole due to the population redistribution.

levels of the excited state are much weaker and do not significantly contribute to the spectrum.[5,3]

The sideholes, whose splittings from the central hole depend linearly on field, result from electronic transitions in which neighboring F nuclear spins accompany the optical electronic transition. The magnetic moment obtained from this field dependence is 4 kHz/G which is just the nuclear moment of the F nucleus. Similar nuclear spin-flip sidebands have been observed[14] in the optical hole spectra of Er^{3+} in $YLiF_4$ and $YAlO_3$. The presence of these spin-flip sidebands make it difficult to see the antiholes at certain fields where the two occur at the same frequency.

The narrow central hole has a width of 40 MHz. This would imply a homogeneous linewidth of 20 MHz if this were homogeneously broadened with $T_2=(\pi\Gamma)^{-1}=16$ ns. However in previous work with paramagnetic ions at low concentrations we have shown that hole linewidths are limited by superhyperfine interactions between the electron spin and the surrounding nuclear moments.[15] Spectral diffusion occurs as the F nuclear spins undergo spin flips producing time-varying local fields at the Eu^{2+} electron spin. Although these spin flips occur slowly because of the frozen-core effect produced by the large electron-spin moment, the full inhomogeneous width of the superhyperfine interaction is accessed over the long (100 ms) time scale of the hole-burning spectrum. The true homogeneous linewidth is therefore probably much less than 20 MHz.

Population hole-burning lifetime

The lifetime of holes formed by hyperfine population storage depends strongly on temperature and magnetic field. Nuclear-spin-lattice relaxation would be only weakly dependent on field and temperature. The mechanism for relaxation among the hyperfine levels involves phonon-induced transitions among the $M_S=-7/2$ and $M_S=-5/2$ electron-spin hyperfine levels. When the electron returns to the $M_S=-7/2$ ground state, it can be in a different hyperfine level, thereby leading to a redistribution of the hyperfine populations. As we show below, evidence for this hole relaxation mechanism comes from the temperature dependence of the hole depth shown in Fig. 3 and the hole-burning curves of Fig. 2. In addition, we have measured the hole lifetime to be 60 s at 77 kG and at a temperature of 2.5 K. The phonon-induced electron-spin transition rate should be proportional to the product of the phonon density of states at the electron-spin transition frequency, $g_{\rm gr}\beta H$, the phonon occupation number, $p=[\exp(g_{\rm gr}\beta H/k_\beta T)-1]^{-1}$, and the square of the matrix element coupling the hyperfine levels of the two spin states. Here $g_{\rm gr}=2$ and k_β is the Boltzmann constant. The hole lifetime is estimated from the data in Figs. 2 and 3. For the data in Fig. 3, holes were burned for 10 s at which point the excitation ceased. The laser was then scanned through the central hole such that the hole was observed 0.5 s after termination of hole burning. The reduction in hole depth as the temperature is increased results from a combination of the reduced initial hole depth due to the refilling of the hole by relaxation during the hole burning and the increased rate of decay of the hole after the hole burning stops. The initial hole depth is approximated from a guess for the hole lifetime and the hole-burning curve of Fig. 2 where the hole lifetime determines how far along the burning curve the hole depth can reach because of refilling. The hole depth 0.5 s after termination of burning is shown in Fig. 3 at several temperatures. The temperatures are that of the bath. The crystal temperature is somewhat higher because it is attached to a cold finger. The temperature of the sample is estimated to be 0.7 K greater than that of the bath temperature. Assuming the hole decays exponentially, a first determination of the hole lifetime can be made from the ratio of the observed hole depth and the estimated initial depth. The estimate of the initial depth was then revised based on the calculated hole lifetime. The process was then iterated until consistency was reached.

In Fig. 9, the hole refilling rate (reciprocal of the hole lifetime) is plotted as a function of the product of H^3 (proportional to the phonon density of states) and the phonon occupation number. Although there are uncertainties in both the temperature and hole decay rate, it is seen that this somewhat limited set of data is consistent with a linear relationship supporting a relaxation mechanism dominated by phonon-induced transitions among the $M_S=-7/2$ and $M_S=-5/2$ electron-spin hyperfine levels.

The long hole lifetimes are a consequence of a combination of a slow phonon-induced electron-spin transition rate (small matrix element) and a small probability of nuclear spin flips accompanying the electronic transitions. To our knowledge this is the only example of population hole burning by storage in the hyperfine levels in a half integral spin system, probably because of the much faster relaxation rates in most half-integer spin systems. However, Macfarlane and Vial[16] have observed population storage in the Zeeman sublevels of Nd^{3+} in very low magnetic fields.

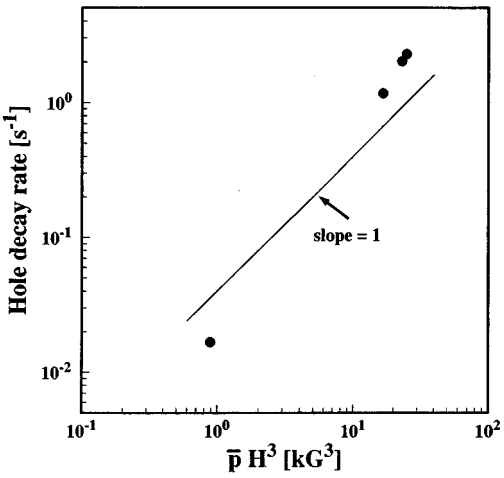

FIG. 9. Hole decay rate as a function of the product of phonon occupation number and H^3. The straight line shows the predicted result for phonon-induced transitions among hyperfine level of the $M_S=-7/2$ and $-5/2$ ground-state electron-spin levels.

Quantum efficiency of hole burning

The hole-burning quantum efficiency is defined as the ratio of the initial rate at which ions are removed from the population by the laser, $[dN_\nu/dt]_{t=0}$, to the absorption rate of photons at the initiation of hole burning, and can be written as[17]

$$\eta=-(h\nu)[dN_\nu/dt]_{t=0}/P\alpha L, \tag{4}$$

where $h\nu$ is the photon energy at 413 nm (6×10^{-19} J), P is the laser power of about 1 mW, α is the sample absorption coefficient at the laser frequency of 413 nm which is approximately 1 cm^{-1}, and L is the sample length of about 1 cm. Because the time development of the hole is not constant but rather its rate decreases with time, η is defined using the initial rate of hole formation. We can reexpress Eq. (4) in terms of the initial rate of change of the transmission using

$$[dN_\nu/dt]_{t=0}=T_0^{-1}[dT/dt]_{t=0}N_0V(\Delta\upsilon_{\rm ion}/\Delta\upsilon_{\rm inh}), \tag{5}$$

where N_0 is the Eu^{2+} density, V is the volume excited by the laser, $\Delta\upsilon_{\rm ion}$ is the effective linewidth of the absorption of a single ion and $\Delta\upsilon_{\rm inh}$ is the inhomogeneous linewidth, about 40 GHz. If the ion had only a single transition, $\Delta\upsilon_{\rm ion}$ would be the homogeneous linewidth.

For hyperfine population hole burning almost all the hole intensity occurs on a single hyperfine transition of an ion so that $\Delta\upsilon_{\rm ion}=20$ MHz (see Fig. 4). From Fig. 2 we see that $[dT/dt]_{t=0}/T_0=0.1/0.1$ s yielding η(population)$\approx10^{-5}$. This implies that an ion must be excited about 10^5 times before it returns to a different hyperfine level of the ground state. As the population in other hyperfine levels increases, backfeeding can occur thereby reducing the rate of hole production since an equilibrium is reached between the forward and backward population redistribution.

For photoionization hole burning, the situation is quite complicated. In the first place, photoionization occurs by a two-step process. The first photon excites the Eu^{2+} ion to the f^6d excited state and the second photon produces photoionization. In addition, all ions do not have the same quantum efficiency since the photoionization rate depends on the proximity of the electron traps. The ions that photoionize first are those for which the released electron can be most easily trapped and have the greatest branching ratio for the electron trapping relative to a return of the election to the initial excited ion. The ions with a lower branching ratio require a greater number of excitations before trapping will occur. In addition, if the number of traps is small, the number of available traps may decrease as the photoionization proceeds. Furthermore, the traps may be photoionized by the 413 nm radiation, returning the electron to the previously photoionized Eu ion.

Because the photoionization is a two photon process, the photoionization efficiency is power dependent, i.e., $[dT/dt]_{t=0}$ in Eq. (5) is not linear in power, as for population hole burning, but should depend on P^2. Rather, we define the efficiency of photoionization from the excited state. For this we write the efficiency as the ratio of the rate of photoionization to the rate of excited-state absorption events

$$\eta=-(h\nu)[dN_\nu/dt]_{t=0}/[P\alpha^*L], \tag{6}$$

where α^* is the excited-state absorption coefficient. The excited-state absorption coefficient can be obtained from the excited-state absorption experiments of Owen, Dorain, and Kobayasi,[18] where, at 413 nm, they find an excited-state extinction coefficient of 4×10^3 l(mole cm)$^{-1}$. In the current experiments, with a power of 1 mW, we estimate N^* (this work)$\cong10^{13}$ cm^{-3} giving $\alpha^*\cong6\times10^{-5}$ cm^{-1}. From the initial rate at which the hole burns we estimate that $T_0^-[dT/dt]_{t=0}=0.1/1000$ s$=10^{-4}$. We also estimate $\Delta\upsilon_{\rm ion}\cong3$ GHz (see Fig. 1). Thus, using Eqs. (5) and (6), we estimate η(photoionization)$\approx2\times10^{-3}$. This is an average initial rate of photoionization for an ion in the $4f^6(^7F_J)5d$ excited state.

Attempts to produce persistent holes in a magnetic field were unsuccessful. In part this may be explained by the reduction of population of the initial state hyperfine level since this level will be depopulated by transient hole burning which, as has been demonstrated, produces deep holes. As a result, in a magnetic field the first step in the two-step photoionization process occurs with reduced probability due to population hole burning.

Thermal stability of persistent holes

Persistent holes at zero magnetic field were found to survive cycling for 5 min at 300 K. The thermal stability was tested in a double-doped sample of CaF_2 containing 0.1% each of Eu and Sm. Hole burning was performed on the $4f^7\rightarrow4f^6(^7F_J)5d$ transition of Eu^{2+} at 413 nm using a pulsed tunable dye laser pumped by a N_2 laser. The dye laser produced 100 μJ pulses of 5 ns duration, 0.1 cm^{-1} (3 GHz) bandwidth, at a repetition rate of 10 Hz. Holes were burned in about 50 pulses focused to a diameter of 2 mm. The holes were detected using a tungsten lamp source and 0.85 m Jarrell Ash spectrometer using 20 μm slits yielding a resolution of 1 cm^{-1}.

The solid curve in Fig. 10 is the absorption before hole burning. The maximum absorption is about 50%. The dashed curve shows the absorption spectrum after three holes were burned in the absorption line. The samples was first cycled to

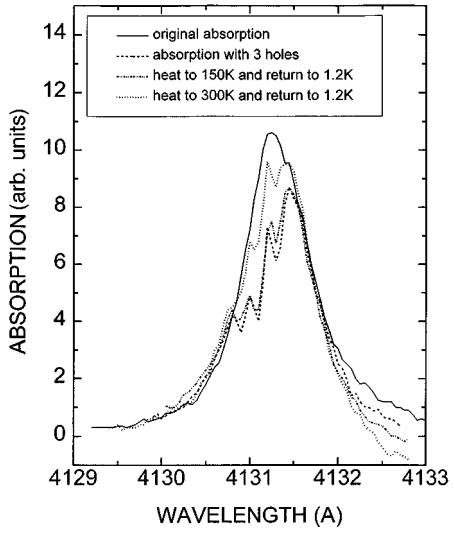

FIG. 10. Absorption spectrum at 1.2 K of the $4f^7(^8S_{7/2}) \rightarrow 4f^6 5d(\Gamma_8)$ zero-phonon transition of Eu^{2+} in CaF_2 containing 0.1% of both Eu^{2+} and Sm^{2+}. The solid curve is the spectrum before hole burning. The dashed curve is the spectrum with three holes burned with a pulsed tunable dye laser. The dot-dash line is the spectrum after cycling the sample for 5 min to 150 K. The dotted spectrum shows a remnant of the hole spectrum after cycling for 5 min to 300 K.

$\cong$150 K for about 5 min with the result that the hole spectrum remained unchanged at 1.5 K as shown by the dot-dash curve. Finally the sample was cycled for 5 min to room temperature as shown by the dotted curve. When the sample was returned to 1.5 K the holes partially survived the temperature cycling but with some loss of depth, as seen in Fig. 10, indicating that the traps are fairly deep. Since the sample is double doped with both ions stable in both the doubly and triply ionized states, we cannot say whether the Eu^{3+} or Sm^{3+} act as the primary electron traps.

CONCLUSIONS

Optical hole burning has been observed for Eu^{2+} ions in CaF_2. Narrow holes were observed in the deep blue part of the spectrum at 413 nm when the laser is tuned to the zero-phonon line of the $4f^7 \rightarrow 4f^6 5d$ transition. Two mechanisms exist for the hole burning. At zero magnetic field, persistent hole burning occurs by photoionization of the Eu^{2+} ions and in a double-doped Eu/Sm sample the electron traps are quite deep. The resulting hole spectrum consists of a narrow spectral feature, whose linewidth is 200 MHz, and broader sideholes whose frequency structure is explained based on the small splitting of the $^8S_{7/2}$ ground state and the hyperfine interactions in both the ground and excited states of the two Eu isotopes.

In a magnetic field exceeding 1 T, a second mechanism is responsible for transient hole burning. This results from the redistribution of population among the hyperfine levels of the ground state. Above 5 T the hole lifetime is minutes. This is an observation of long-lived population hole burning in an ion with half integer spin. The hole spectrum results from the hyperfine structure in the ground and excited states. The temperature dependence of the hole lifetime supports the idea that the hole decay occurs by phonon-induced transitions to the higher electron spin levels with a small probability of accompanying nuclear spin flips. The 40 MHz observed hole width is probably inhomogeneously broadened by superhyperfine interactions. As a result, the expected very narrow homogeneous linewidth ($\ll$20 MHz) when combined with the strong coupling of the transition to the light, make this an interesting candidate for optical signal processing providing the efficiency can be enhanced.

Both mechanisms occur with low efficiency. Population hole burning occurs with an efficiency of about 10^{-5} for a magnetic field of about 8 T. Persistent hole burning at zero field due to photoionization is a two-step process. The second step, which occurs by excited-state absorption, has an efficiency of about 2×10^{-3}. This efficiency must surely be sample dependent, controlled by the availability of stable traps, most probably Eu^{3+} ions, whose concentration can be controlled in the crystal preparation.

The occurrence of long-lived transient holes in this $S=7/2$ ion indicates that holes with long lifetimes should be expected in other half integral electron-spin systems at high magnetic fields. For example, the $S=7/2$ ground state of Gd^{3+} might show similar behavior.

ACKNOWLEDGMENTS

We acknowledge the support of the National Science Foundation, Grants No. DMR-9015468 and DMR-9321052. One of us (D.M.B.) also thanks Davidson College and the Office of Vice President for Research at the University of Georgia for partial support. We also thank Dr. N. Sokolov of the Ioffe Institute for the 0.001% $Eu^{2+}CaF_2$ sample and Jan Schmidt for helpful comments.

[1] R. M. Macfarlane and R. M. Shelby, in *Spectroscopy of Solids Containing Rare Earth Ions*, edited by A. A. Kaplyanskii and R. M. Macfarlane (North-Holland, Amsterdam, 1987), pp. 62–67.

[2] A. A. Kaplyanskii and P. P. Feofilov, Opt. Spectrosc. (USSR) **13**, 129 (1962).

[3] B. P. Zakharchenya, I. B. Rusanov, and A. Ya. Ryskin, Opt. Spectrosc. (USSR) **18**, 563 (1965).

[4] A. A. Kaplyanskii and A. K. Przhevuskii, Opt. Spectrosc. (USSR) **19**, 331 (1965).

[5] P. Kisliuk, H. H. Tippens, and C. A. Moore, Phys. Rev. **171**, 336 (1968).

[6] J. M. Baker, B. Bleaney, F. R. S. and W. Hayes, Proc. R. Soc. London **247**, 141 (1958).

[7] J. M. Baker and F. I. B. Williams, Proc. R. Soc. London Sect. A **257**, 283 (1962).

[8] L. L. Chase, Phys. Rev. B **2**, 2308 (1970).

[9] P. P. Feofilov, Opt. Spektrosc. (USSR) **1**, 992 (1956).

[10] C. Pedrini, F. Rogemond, and D. S. McClure, J. Appl. Phys. **59**,

1196 (1986).
[11] P. P. Feofilov, Opt. Spectrosk. **12**, 531 (1962), **12**, 296 (1962); B. Welber, J. Chem. Phys. **42**, 4262 (1965).
[12] A. Abragam and B. Bleaney, *Electron Paramagnetic Resonance of Transition Ions* (Dover, New York, 1970).
[13] B. Bleaney, Proc. Phys. Soc. London **73**, 939 (1959).
[14] R. Wannemacher, R. M. Macfarlane, Y. P. Wang, D. Sox, D. Boye, and R. S. Meltzer, J. Lumin. **48/49**, 309 (1991).
[15] R. Wannemacher, R. S. Meltzer, and R. M. Macfarlane, J. Lumin. **45**, 307 (1990).
[16] R. M. Macfarlane and J. C. Vial, Phys. Rev. B **36**, 3511 (1987).
[17] W. E. Moerner, A. R. Chraplyvy, A. J. Sievers, and R. H. Silsbee, Phys. Rev. B **12**, 7244 (1983).
[18] J. F. Owen, P. B. Dorain, and R. Kobayasi, J. Appl. Phys. **52**, 1216 (1981).